Monthly and fortnightly tidal variations of the Earth's rotation rate predicted by a TOPEX/POSEIDON empirical ocean tide model

Shailen D. Desai
Jet Propulsion Laboratory, California Institute of Technology, Pasadena, California

John M. Wahr
Department of Physics and Cooperative Institute for Research in Environmental Sciences, University of Colorado, Boulder, Colorado

Short title: MM AND MF TIDAL VARIATIONS IN EARTH'S ROTATION RATE

Abstract. Empirical models of the two largest constituents of the **long-period ocean tides**, the monthly and the fortnightly constituents, are estimated from repeat cycles 10 to 210 of the **TOPEX/POSEIDON** (T/P) mission. These models are first validated with tide gauge observations which show residual variances with the T/P-derived models that are of the order of 2-3 mm^2 for both the monthly and fortnightly constituents, and which are smaller than residual variances from respective equilibrium models of these long-period ocean tides. These empirical models are used to predict the contribution that they each have on tidal variations of the **Earth's rotation rate.** For tidal variations in UT1 these contributions are predicted to be of the order of 0.1 ms with a scatter of the order of 8 and 3 μs for the monthly and fortnightly ocean tides, respectively.

Introduction

The long-period tidal potential causes axisymmetric tidal deformations in the solid Earth that translate directly into changes in the polar moment of inertia of the Earth. To conserve the Earth's angular momentum these deformations cause the first order contribution to long-period tidal variations of the Earth's rotation rate, and are known to better than 1% [*Yoder et al.,* 1981]. Similarly, the long-period ocean tides cause a second order contribution to long-period tidal variations of the Earth's rotation rate both from changes in the polar moment of inertia of the Earth and from changes in the relative angular momentum of the oceans with respect to the solid Earth. There is also a third order contribution that is caused by the anelasticity, or damped response, of the Earth's mantle to the long-period tidal potential. The magnitude of this contribution remains uncertain but can be inferred from observed long-period tidal variations of the Earth's rotation rate given adequate knowledge of the respective ocean tide contributions [*Wahr and Bergen,* 1986; *Desai,* 1996; *Dickman and Nam,* 1998].

Predictions of the contribution from the long-period ocean tides have been limited by the fact that the actual response of the long-period ocean tides is a subject of continuing investigation in large part because of the lack of accurate global observations. The long-period ocean tides have sometimes been considered to be of sufficiently long period to have a response that coincides, or is in equilibrium, with the forcing equipotential surface [*Agnew and Farrell,* 1978]. However, most hydrodynamic analyses [e.g. *Miller et al.,* 1993] suggest that the two principal long-period ocean tide constituents, the monthly M_m and the fortnightly M_f constituents, should have departures from equilibrium that are significant for Earth rotation rate predictions.

TOPEX/POSEIDON (T/P) altimetry provides a unique opportunity to provide almost global observations of the long-period ocean tides because of the relatively small measurement accuracies that are of the the order of 4-5 cm, and because of the long duration of available data which now spans 5 years. *Desai* *and Wahr* [1995] and Desai [1996], hereinafter referred to as DW95 and D96, developed almost global empirical models of the M_m and M_f ocean tides from the first 2-3 years of T/P data. The preliminary results from DW95 and D96 appeared to contain short wavelength noise in the long-period ocean tide estimates. Error analyses both by D96 and *Desai et al.* [1997], hereinafter referred to as DWC97, suggested that longer durations of T/P data would provide improved estimates of the M_m and M_f ocean tides, particularly by reducing contamination from general ocean circulation noise.

Here, updated T/P-derived empirical models of the M_m and M_f ocean tides are first validated with tide gauge comparisons and then used to predict their respective contributions to tidal variations of the Earth's rotation rate. These M_m and M_f ocean tide height models are developed with similar strategies to those described in DW95 and D96 and therefore not repeated here. The most important difference is that while DW95 and D96 estimated models that respectively used data from repeat cycles 10-78 and 10-110 of the T/P mission, results presented here use models that have been updated to use almost twice as long a data duration by using repeat cycles 10-210. The effect on the Earth rotation rate predictions from the inclusion of longer durations of altimetric data into the empirical tide models are also illustrated.

Tide Gauge Comparisons

Miller et al. [1993], hereinafter referred to as MLH93, used long durations (3 to 65 years) of tide gauge data to provide 17 M_m and 24 M_f tide gauge observations concentrated in the Pacific Ocean. A global set of M_m and M_f tide gauge observations would certainly be more useful to validate the T/P models, but such a data set is not easily available because accurate tide gauge observations of the M_m and M_f oceans tides require long data records to reduce leakage from oceanographic noise at these long periods. Nevertheless, the MLH93 observations provide some degree of validation of the T/P-derived M_m and M_f models and also help to quantify improvements in these models. For reasons already outlined in DWC97 only a subset of 14 M_m and 23 M_f tide gauge observations from MLH93 are used for comparisons to the T/P empirical models, and these results are provided in Table 1. The two equilibrium models also compared in Table 1 differ in that the self-consistent equilibrium model, hereinafter referred to as the SCEQU model, considers the self-gravitation and load deformations of the equilibrium ocean tides while the classical equilibrium model, hereinafter referred to as the CEQU model, does not [*Agnew and Farrell,* 1978]. Table 1

Neither of the equilibrium models have a quadrature component and therefore cannot explain any of the observed quadrature tide gauge variance, while the T/P cycle 210 model explains more than 60% of the observed quadrature variance. Including an additional 100 repeat cycles of T/P data into the empirical models reduces the total tide gauge residual variances from 4.3 to 2.3 mm^2 for M_m and 4.5 to 2.3 mm^2 for M_f. This represents a decrease from 26.1 to 13.9%, and 10.9 to 5.6% of the respective M_m and M_f observed tide gauge variance.

Theory

Tidal variations of the Earth's rotation rate are interpreted either by variations in the length of day $\Delta\Lambda$, or in Universal time UT1 with respect to the reference atomic time standard TAI. The zonal response coefficient κ also serves as a convenient parameter to observe the frequency dependence of long-period tidal variations of the Earth's rotation rate, since it essentially normalizes $\Delta\Lambda$ by the respective long-period tide potential amplitudes [e.g. *Nam and Dickman,* 1990]. From *Gross* [1992],

$$\begin{aligned} \frac{d(\text{UT1-TAI})}{dt} &= -\frac{\Delta\Lambda(t)}{\Lambda_0} = \kappa\frac{MRH_{20j}}{3C}\left(\frac{5}{\pi}\right)^{1/2} \\ &= \frac{1}{C_m\Omega}[0.756\Omega c_{33}(t) + h_3(t)] \end{aligned} \tag{1}$$

where the polar moment of inertia of the whole Earth and the mantle, and the Earth's mean rotation rate, nominal length of day, mean radius, and mass are respectively defined by C, C_m, Ω, Λ_0, R, and M. The long-period tide potential amplitudes H_{20j} use conventions from *Cartwright and Taylor* [1971] with values of -3.518 and -6.661 cm for $\mathrm{M_m}$ and $\mathrm{M_f}$, respectively.

The mass contribution is defined by changes in the Earth's polar moment of inertia c_{33} caused by the ocean tide heights $\zeta(\theta, \lambda, t)$ at colatitude θ and longitude λ, and the motion contribution is defined by the relative angular momentum of the ocean tides h_3 which is caused by the eastward tidal currents $v(\theta, \lambda, t)$.

$$c_{33}(t) = \rho_w R^4 \int_0^{2\pi} \int_0^{\pi} \zeta(\theta, \lambda, t) \sin^3 \theta d\theta d\lambda \tag{2}$$

$$h_3(t) = \rho_w R^3 \int_0^{2\pi} \int_0^{\pi} H(\theta, \lambda) v(\theta, \lambda, t) \sin^2 \theta d\theta d\lambda \tag{3}$$

It is assumed that the oceans have a mean density of $\rho_w = 1.035 \mathrm{g/cm^3}$ and that the tidal currents are constant through the column of water of depth $H(\theta, \lambda)$. Here, the tidal currents are approximated through the application of finite differences of the ocean tide height models into frictionless Laplace tidal equations, similar to the procedure adopted by *Chao et al.* [1995] on T/P tide height models of the diurnal and semidiurnal ocean tides. The T/P observations are limited to within the latitudes of ±66° and it is assumed here that the tidal response (heights and currents) in the unsampled latitudes poleward of ±66° is zero, or modeled by the CEQU, SCEQU, or *Schwiderski* [1980] models. These global models are then respectively referred to as the T/P only, T/P+CEQU, T/P+SCEQU, and T/P+SCH models.

Results and Discussion

For variations in UT1 the inphase $\mathrm{UT_S}$ and quadrature $\mathrm{UT_C}$ components are defined here as:

$$\text{UT1-TAI} = \mathrm{UT_S} \sin(\phi_{20j}(t)) + \mathrm{UT_C} \cos(\phi_{20j}(t)) \tag{4}$$

where $\phi_{20j} = (\omega_{20j} t + \beta_{20j} + \delta_{20j}\pi)$ is the astronomical argument with the conventions from equations (3), (4), and (5) of DW95 used to define ω_{20j}, β_{20j}, and δ_{20j}. Figure 1 Figure 1 illustrates the predicted M_m and M_f ocean tide contributions to variations in κ using T/P+SCH models that successively include 10 additional repeat cycles of altimetric data when estimating the models, beginning with a model that uses repeat cycles 10-80 and ending with a model that uses repeat cycles 10-210. Table 2 then provides values of the predicted UT1 variations from the various forms of the M_m and M_f cycle 210 ocean tide models mentioned above. This table also provides statistics (mean and standard deviation) of the scatter in the predicted UT1 variations from the cycle 150 to cycle 210 T/P+SCH models. For comparison, the CEQU and SCEQU model predictions computed by D96 are also shown, noting that by definition the equilibrium long-period ocean tide models do not have a quadrature mass contribution or any motion contribution. Table 2

Of course, the inphase mass contributions represent the largest contribution because c_{33} is proportional to the second degree spherical harmonic component of the ocean tides and the long-period ocean tides are dominated by an inphase second degree zonal spherical harmonic component. Long-period ocean tide theory predicts that these ocean tides should have smaller relative departures from equilibrium with increasing tidal period. Results presented here are consistent with this theory for the predicted mass contributions, with the T/P+SCH M_m mass contributions being closer to equilibrium than those for M_f in both the inphase and quadrature components. However, the predicted T/P+SCH M_m quadrature motion contributions appear to have unrealistically large values. This is likely to be caused by the fact that the T/P M_m tide height models continue to have extensive short wavelength features that are possibly amplified when constructing finite differences for the computation of the tidal currents. Notice also that the predicted M_f quadrature motion contributions appear to be slowly decreasing as the T/P empirical models are updated with new data. In general, the M_m mass and motion contributions both have a larger 1σ scatter, by at least a factor of three, than the respective M_f contributions. This is likely to be the result of the M_m ocean tide having twice the period and half the amplitude of the M_f ocean tide and therefore being much more susceptible to ocean circulation noise at these long periods. Of course, most of the relatively large scatter in the M_m predictions arises from the motion contributions.

The scatter in the T/P+SCH predictions might be considered to be a quantification of the errors in the Earth rotation rate predictions that specifically arise from errors in the T/P empirical models themselves. A comparison of the UT1 predictions with the four various assumptions about the tidal response in the unsampled polar latitudes then provides some measure of errors caused by uncertainties in the tidal response in these latitudes. Note that a nonzero tide height response in the polar latitudes contributes almost 30μs to both the M_m and M_f mass predictions, which is significant in comparison to the scatter of the respective rotation rate predictions. The substitution of the CEQU or SCEQU tides for the SCH tides in the unsampled latitudes has a relative small effect of the order of 3-6 μs on the M_m predictions compared to 10-15 μs for M_f. However, tide gauge comparisons as well as comparisons of the tidal response between the various models in regions sampled by T/P suggest that the M_m and M_f responses in the unsampled polar latitudes are probably best approximated by the CEQU and SCH models, respectively.

Tide gauge residual variances with the T/P M_m model continue to decrease with incoming T/P data, particularly in the quadrature component, and use of incoming data should help to reduce the magnitude of the short wavelength errors in the M_m empirical models. Future updates of the T/P empirical models are therefore likely to only provide significant improvements to the M_m motion contributions, but will also provide small improvements to predicted M_f motion and M_m mass contributions. However, Earth rotation rate predictions from T/P empirical models are still limited by the uncertainties in the tidal response in those latitudes not sampled by T/P. Reducing these uncertainties will probably require improved hydrodynamic analyses of the tidal response in these latitudes.

Acknowledgments. Early portions of this work were supported by the TOPEX project at the Jet Propulsion Laboratory under contract 958126 to the University of Colorado. S.D. was also supported by a contract from NASA to the Jet Propulsion Laboratory.

References

Agnew, D. C., and W. E. Farrell, Self-consistent equilibrium ocean tides, *Geophys. J. R. Astron. Soc., 55*, 171-181, 1978.

Cartwright, D. E., and R. J. Taylor, New computations of the tide-generating potential, *Geophys. J. R. Astron. Soc., 23*, 45-74, 1971.

Chao, B. F., R. D. Ray, and G. D. Egbert, Diurnal/ Semidiurnal oceanic tidal angular momentum: Topex/Poseidon models in comparison with Earth's rotation rate, *Geophys. Res. Lett., 22*, 1993-1996, 1995.

Desai, S. D., Ocean tides from TOPEX/POSEIDON altimetry with some geophysical applications, Ph.D. thesis, Univ. of Colo., Boulder, 1996.

Desai, S. D. and J. M. Wahr, Empirical ocean tide models estimated from TOPEX/POSEIDON altimetry, *J. Geophys. Res., 100*(C12), 25,205-25,228, 1995.

Desai, S. D., J. M. Wahr, and Y. Chao, Error analysis of empirical ocean tide models estimated from TOPEX/POSEIDON altimetry, *J. Geophys. Res., 102*(C11), 25,157-25,172, 1997.

Dickman, S. R., and Y. S. Nam, Constraints on Q at long periods from Earth's rotation, *Geophys. Res. Lett., 25*(2), 211-214, 1998.

Gross, R. S., Correspondence between theory and observations of polar motion, *Geophys. J. Int., 109*, 162-170, 1992.

Miller, A. J., D. S. Luther, and M. C. Hendershott, The fortnightly and monthly tides: Resonant Rossby waves or nearly equilibrium gravity waves?, *J. Phys. Oceanogr., 23*, 879-897, 1993.

Nam, Y. S., and S. R. Dickman, Effects of dynamic long-period ocean tides on changes in Earth's rotation rate, *J. Geophys. Res., 95*(B5), 6751-6757, 1990.

Schwiderski, E. W., Ocean tides, II, A hydrodynamical interpolation model, *Mar. Geod., 3*, 219-255, 1980.

Wahr, J. M. and Z. Bergen, The effects of mantle anelasticity on nutations, Earth tides, and tidal variations in rotation rate, *Geophys. J. R. Astron. Soc., 87*, 633-668, 1986.

Yoder, C. F., J. G. Williams, and M. E. Parke, Tidal variations of Earth rotation, *J. Geophys. Res., 86*(B2), 881-891, 1981.

S. D. Desai, Jet Propulsion Laboratory, 4800 Oak Grove Drive, M/S 238-600, Pasadena, CA 91101. (e-mail: shailen.desai@jpl.nasa.gov)

J. M. Wahr, Department of Physics, CB 390, University of Colorado, Boulder, CO 80309-0390, (e-mail: wahr@lemond.colorado.edu)

Received October 27, 1998; revised 1999; accepted 1999.

Submitted for review by *Geophysical Research Letters*, 1998.

Figure 1. Predicted mass and motion contributions of the T/P+SCH M_m and M_f ocean tide models to tidal variations of the Earth's rotation rate in the form of the zonal response coefficient κ, as a function of the duration of T/P data included into the empirical models. M_m and M_f variations are shown with the plus (+) and asterisk (*) symbols, respectively. Also shown are the values of κ for the self-consistent and classical equilibrium models, SCEQU and CEQU, respectively.

Table 1. Root-Mean-Square of Differences Between 14 M_m and 23 M_f Tide Gauge Observations from *Miller et al.* [1993] and the Classical Equilibrium (CEQU), Self-Consistent Equilibrium (SCEQU), and the TOPEX/POSEIDON (T/P) Ocean Tide Models.

Model	M_m Tide			M_f Tide		
	I	Q	T	I	Q	T
Observed [a]	5.28	2.22	4.05	8.20	3.83	6.40
SCEQU	2.04	2.22	2.13	4.55	3.83	4.21
CEQU	1.37	2.22	1.84	2.52	3.83	3.24
T/P Cycle 110 [b]	2.19	1.94	2.07	2.32	1.87	2.11
T/P Cycle 210 [c]	1.66	1.34	1.51	1.57	1.47	1.52

Units are millimeters. I is inphase, Q is quadrature, and T is total, and $T = ((I^2 + Q^2)/2)^{1/2}$.

[a]No model differenced with tide gauge observations

[b]Values are from *Desai* [1996] using a model estimated from T/P cycles 10-110.

[c]Values are from a model estimated from T/P cycles 10-210.

Table 2. Contribution of the M_m and M_f Ocean Tides to Tidal Variations in UT1

	M_m						M_f					
	Mass		Motion		Total		Mass		Motion		Total	
Model	UT_s	UT_c	UT_s	UT_c	UT_s	UT_c	UT_s	UT_c	UT_s	UT_c	UT_s	UT_c
CEQU	-114.7	0.0	0.0	0.0	-114.7	0.0	-107.7	0.0	0.0	0.0	-107.7	0.0
SCEQU	-135.3	0.0	0.0	0.0	-135.3	0.0	-127.0	0.0	0.0	0.0	-127.0	0.0
T/P only	-91.2	9.1	-4.3	48.4	-95.5	57.4	-79.7	19.1	-0.6	16.7	-80.3	35.8
T/P+CEQU	-120.8	9.1	-4.3	48.4	-125.1	57.4	-107.5	19.1	-0.6	16.7	-108.1	35.8
T/P+SCEQU	-125.4	9.1	-4.3	48.4	-129.7	57.4	-111.8	19.1	-0.6	16.7	-112.4	35.8
T/P+SCH [a]	-118.9	6.4	-4.7	48.1	-123.6	54.6	-97.7	30.8	-0.3	16.9	-98.1	47.7
T/P+SCH [b]	-116.8	4.6	-2.1	40.4	-118.9	45.0	-98.2	31.4	-3.2	19.1	-101.5	50.6
	(2.0)	(1.6)	(5.8)	(6.4)	(7.5)	(7.9)	(0.4)	(0.5)	(1.7)	(2.2)	(1.9)	(2.5)

Units are microsec.

[a]Values are from the cycle 210 T/P+SCH model.

[b]Values are computed as the mean of the UT1 variations predicted from the cycle 150-210 T/P+SCH models. Values in ()s are the standard deviations about the mean values.

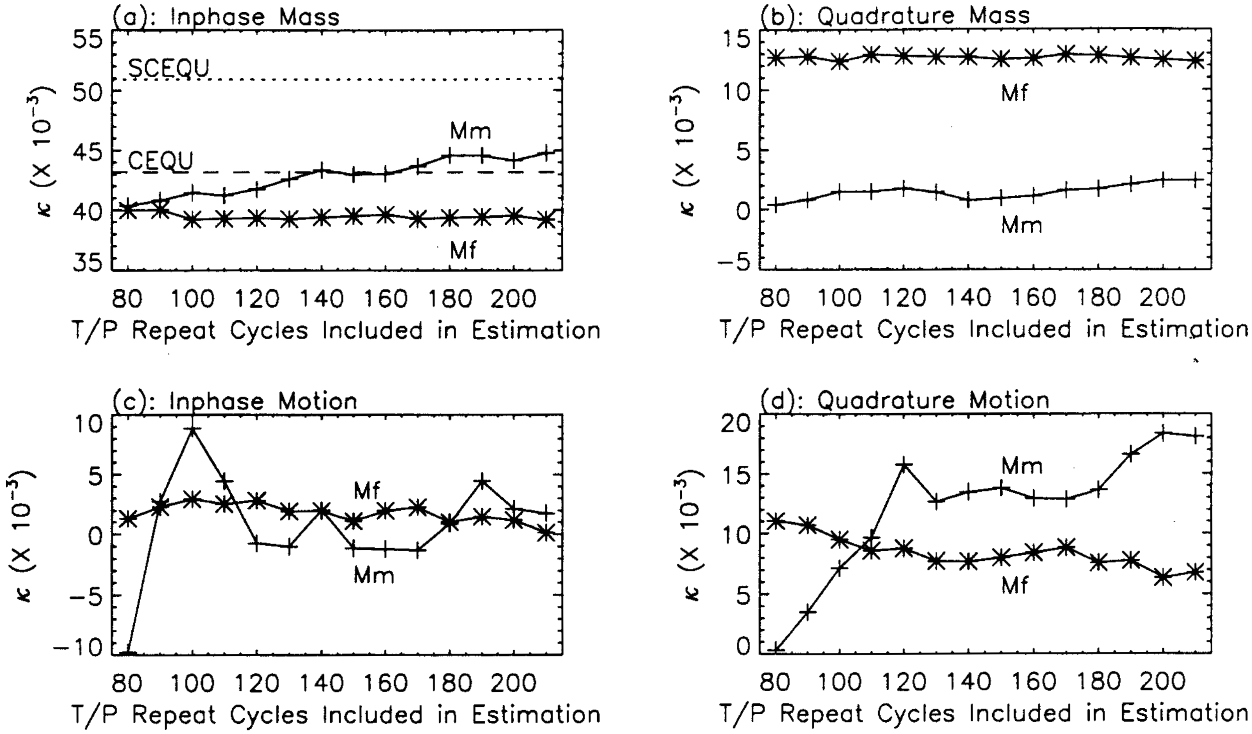
(a): Inphase Mass
SCEQU
CEQU
Mm
Mf
κ (X 10⁻³)
55
50
45
40
35
80 100 120 140 160 180 200
T/P Repeat Cycles Included in Estimation
(b): Quadrature Mass
Mf
Mm
κ (X 10⁻³)
15
10
5
0
−5
80 100 120 140 160 180 200
T/P Repeat Cycles Included in Estimation
(c): Inphase Motion
Mf
Mm
κ (X 10⁻³)
10
5
0
−5
−10
80 100 120 140 160 180 200
T/P Repeat Cycles Included in Estimation
(d): Quadrature Motion
Mm
Mf
κ (X 10⁻³)
20
15
10
5
0
80 100 120 140 160 180 200
T/P Repeat Cycles Included in Estimation

Figure 1